



Deposited via The University of York.

White Rose Research Online URL for this paper:

<https://eprints.whiterose.ac.uk/id/eprint/3424/>

---

**Article:**

Gao, T.R., Yang, D.Z., Zhou, S.M. et al. (2007) Hysteretic behavior of angular dependence of exchange bias in FeNi/FeMn bilayers. Physical Review Letters. 057201. -. ISSN: 1079-7114

<https://doi.org/10.1103/PhysRevLett.99.057201>

---

**Reuse**

Items deposited in White Rose Research Online are protected by copyright, with all rights reserved unless indicated otherwise. They may be downloaded and/or printed for private study, or other acts as permitted by national copyright laws. The publisher or other rights holders may allow further reproduction and re-use of the full text version. This is indicated by the licence information on the White Rose Research Online record for the item.

**Takedown**

If you consider content in White Rose Research Online to be in breach of UK law, please notify us by emailing [eprints@whiterose.ac.uk](mailto:eprints@whiterose.ac.uk) including the URL of the record and the reason for the withdrawal request.

*promoting access to White Rose research papers*



**Universities of Leeds, Sheffield and York**  
**<http://eprints.whiterose.ac.uk/>**

---

This is an author produced version of a paper to be/subsequently published in **Physical Review Letters**. (This paper has been peer-reviewed but does not include final publisher proof-corrections or journal pagination.)

White Rose Research Online URL for this paper:  
<http://eprints.whiterose.ac.uk/3424>

---

**Published paper**

Gao, T. R., Yang, D. Z., Zhou, S. M., Chantrell, R., Asselin, P., Du, J. and Wu, X. S. (2007) Hysteretic behavior of angular dependence of exchange bias in FeNi/FeMn bilayers. *Physical Review Letters*, 99 (5). Art. No. 057201.

---

# Hysteretic behavior of angular dependence of exchange bias in FeNi/FeMn bilayers

T. R. Gao, D. Z. Yang, and S. M. Zhou

*The State Key Lab for Advanced Photonic Materials Devices and Department of Physics,  
Fudan University, Shanghai 200433, China*

R. Chantrell

*Physics Department, The University of York, York, YO10 5 DD, UK*

P. Asselin

*Seagate Research, 1251 Waterfront Place, Pittsburgh 15222, USA*

J. Du and X. S. Wu

*National Laboratory of Solid State Microstructures,  
Nanjing University, Nanjing 210093, China*

(Dated: September 8, 2007)

## Abstract

For FeNi/FeMn bilayers, the angular dependence of exchange bias shows hysteresis between clockwise and counterclockwise rotations, as a new signature. The hysteresis decreases for thick antiferromagnet layers. Calculations have clearly shown that the orientation of antiferromagnet spins also exhibits hysteresis between clockwise and counterclockwise rotations. This furnishes an interpretation of the macroscopic behavior of the ferromagnetic layer in terms of the thermally driven evolution of the magnetic state of the antiferromagnet layer.

PACS numbers: 75.30.Et, 75.30.Gw, 75.60.Jk

Among many key questions of ex- spins on the EB is difficult to clarify due change bias (EB) in ferromagnet to the zero net magnetization in the AFM (FM)/antiferromagnet (AFM) bilayers, layer [7–10]. It is often inferred indirectly the important role of AFM spins has been through the motion of the FM magnetization studied extensively both theoretically and with the help of either micro-magnetic or experimentally [1–6]. The effect of AFM classical Heisenberg models [2, 3]. Re-

ported results often disagree on the effect of AFM spins on asymmetrical hysteresis loops [2, 3, 9].

Although the angular dependence of EB (ADEB), specifically the exchange field  $H_E$  and the coercivity  $H_C$ , has been studied extensively, no special consideration has been made of the sense of rotation of the applied magnetic field  $H_a$  [11]. It is assumed *a priori* that the ADEB is identical for clockwise (CW) and counterclockwise (CCW) rotations. For FM/AFM bilayers, however, rotational hysteresis of torque between CW and CCW rotations, often exists even for  $H_a$  larger than the saturation field of the FM layer, because the exchange field acting on AFM spins is smaller than the saturation field of the AFM layer [12, 13]. Thus we can surmise a similar effect on the ADEB between CW and CCW rotations. In this Letter, we reported on hysteresis of the ADEB between CW and CCW rotations. It decreases with increasing AFM layer thickness  $t_{AFM}$ . Calculations show that thermally activated irreversible transitions of the AFM spins are responsible for hysteresis of the ADEB.

A 1 cm  $\times$  5 cm bilayer of  $Fe_{20}Ni_{80}(=FeNi)(3 \text{ nm})/Fe_{50}Mn_{50}(=FeMn)$  was deposited on Si(100) at ambient temperature by DC magnetron sputtering from FeNi and FeMn composite targets. The base

pressure was  $2 \times 10^{-5}$  Pa and the Ar pressure 0.33 Pa during deposition. Before deposition of the bilayer, a 30 nm thick Cu buffer was prepared to stimulate the EB [14]. Finally, another 30 nm thick Cu layer was used to avoid oxidation. Deposition rates of FeNi, FeMn, and Cu layers were 0.3, 0.1, and 0.2 nm/s, respectively. In order to avoid the run-to-run error, the FeMn layer takes a wedged shape across the distance of 5 cm. Each location along the wedge direction corresponds to a specific  $t_{AFM}$ . During deposition, a magnetic field of about 130 Oe was applied parallel to the film plane to induce the EB. Similar fabrication procedure was described elsewhere [15].

X-ray diffraction showed intense and weak peaks at  $2\theta = 43.3^\circ$  and  $50.6^\circ$ , corresponding to (111) and (200) preferred orientations of Cu, FeMn, and FeNi layers, respectively. Apparently, constituent layers are polycrystalline with texture. Before magnetic measurements, the specimen was cut into small pieces along the wedge direction prepared at the same time but varying in  $t_{AFM}$ . No field-cooling was made to avoid morphology degradation at the FM/AFM interface. With a vector vibrating sample magnetometer,  $m_x$  and  $m_y$  were measured, as components of the magnetic moment parallel and perpendicular to  $H_a$ , respectively, where  $H_a$ ,  $m_x$ , and  $m_y$  are parallel

to the film plane, and  $m_x$  corresponds to conventional hysteresis loops. At left and right coercivity, where  $m_x = 0$ ,  $m_y$  has maximal values, namely,  $m_{y-L}$  and  $m_{y-R}$ . We define  $m_{y-AVE} = (m_{y-R} + m_{y-L})/2$  and the asymmetry factor  $\delta = (\text{abs}(m_{y-R}) - \text{abs}(m_{y-L})) / (\text{abs}(m_{y-R}) + \text{abs}(m_{y-L}))$ . During measurements of angular dependence of hysteresis loops,  $H_a$  was set to zero during the rotation of samples. All measurements were performed at room temperature.

Figure 1 shows angular dependence of  $H_E$ ,  $H_C$ ,  $m_{y-AVE}$ , and  $\delta$  for typical FeNi/FeMn bilayer with CW and CCW rotations.  $\phi_H$  is the orientation of  $H_a$ ,  $\phi_H = 0$  defined as the direction at which  $H_E$  in CW rotation has its maximum negative value. Apparently,  $H_C$ ,  $m_{y-AVE}$ , and  $\delta$  have different angular dependence for CW and CCW rotations. For example,  $\phi_H$  is different for  $m_{y-AVE} = 0$  between CW and CCW rotations. The angular difference is defined as  $\Delta\phi_H$ , as shown in Fig. 1(c). It equals 28 degrees for  $t_{AFM}=10$  nm. As shown in Fig. 1(a),  $H_E$  has almost the same angular dependence for CW and CCW rotations, which will be analyzed below.

As discussed below, the results in Fig. 1 are caused by the hysteresis of ADEB. In order to verify this, firstly another CW rotation was measured *directly* after one cycling of CW and CCW rotations. It

is found that the ADEB for the second CW rotation is almost the same as that of the first. Secondly,  $\Delta\phi_H$  is shown to be independent of the increment of  $\phi_H$  between neighboring hysteresis loops. Finally, the ADEB of CW and CCW rotations was measured within different  $\phi_H$  regimes. As shown in Fig. 2(a), the angular dependence of  $m_{y-AVE}$  is reversible for CW and CCW rotations for small  $\phi_H$  ranges. However, it is irreversible for larger  $\phi_H$  regimes, as shown in Fig. 2(b). Unambiguously, the hysteretic behavior of the ADEB is demonstrated.

Figure 3(a) shows that  $H_C$  changes non-monotonically with  $t_{AFM}$ , while  $H_E$  changes monotonically, similar to previous results [1]. Figure 3(b) shows that  $\Delta\phi_H$  also changes non-monotonically with  $t_{AFM}$ . For bilayers with small  $t_{AFM}$ , and also for single FM layers,  $\Delta\phi_H = 0$ . For  $t_{AFM} > 6$  nm,  $\Delta\phi_H$  sharply increases with increasing  $t_{AFM}$  to reach a maximum and then decreases.

We have developed a computational model of the hysteretic phenomenon, including thermal activation within the AFM layer. The FM and AFM layers are modelled as a granular microstructure produced using a Voronoi construction (see for example [16]). Each layer has the *same* microstructure, which describes realistic systems where columnar growth is continuous across interfaces. The AFM grains are consid-

ered exchange-decoupled while neighboring FM-FM and FM-AFM grains are strongly exchange-coupled. The AFM layer is treated using a kinetic Monte Carlo algorithm [17]. The *coherent* reversal of AFM spins is governed by thermally activated processes, i.e., the grains are allowed to reverse with a probability  $p_{sw}$  given by the Arrhenius-Néel law [18]. In view of the hysteretic behavior of the ADEB, we consider samples with  $t_{AFM}$  much smaller than the domain wall thickness and thus neglect planar domain wall in the AFM layer [19].  $p_{sw}$  is determined by the intrinsic energy barrier, determined by the local anisotropy energy  $E_{anis}$ , and the exchange field from the FM layer.  $E_{anis} = a_0 t_{AFM} K_{AFM} \sin^2 \phi_{AFM}$ , where  $\phi_{AFM}$  is the angle between AFM spins and the easy axis. The anisotropy constant  $K_{AFM}$  is single valued and the lateral area of AFM grains  $a_0$  has a lognormal distribution with a standard deviation  $\sigma = 0.3$ . The easy axes of the AFM grains are assumed planar randomly orientated. The interlayer exchange energy is [20]  $E_{exch} = -a_0 c_0 J_{int} \hat{S}_{FM} \cdot \hat{S}_{AFM}$ , where  $J_{int}$  is the interface exchange coupling constant,  $\hat{S}_{FM}$  and  $\hat{S}_{AFM}$  are the unit vectors of the FM and AFM moments at the interface, respectively. The contact fraction  $c_0$  represents the net imbalance of two sublattice magnetizations contacting the FM layer. Determination of stationary

states from the total free energy  $E_{exch} + E_{anis}$  allows calculation of the energy barrier, from which  $p_{sw}$  is determined. The FM layer is treated in a standard micromagnetic approach with the cell size being the grain size. The FM grains are coupled with the bulk exchange energy. The magnetic equilibrium state is determined by minimizing the Gibbs free energy, which includes Zeeman, exchange, anisotropy, magnetostatic terms, and interlayer exchange coupling energy. Minimization of the energy is achieved using a Conjugate Gradient method. With strong exchange-coupling between FM grains, nonuniform magnetization reversal process should occur.

Figures 4(a)-4(d) show calculations for a system with a median AFM grain size of 5 nm and  $\sigma = 0.3$ ,  $t_{AFM}=7$  nm,  $t_{FM}=3$  nm,  $K_{AFM} = 4 \times 10^6$  erg/cc, and  $K_{FM} = 5 \times 10^3$  erg/cc. For simplicity, it is assumed that  $M_{FM} = M_{AFM}=750$  emu/cc and the exchange field between FM-FM and FM-AFM grains is 500 Oe. The present model reproduces major features of the experimental results, except for  $H_E$ , for reasons to be discussed shortly.

The hysteresis of the ADEB can be explained qualitatively. Consider a hysteresis loop for the FM layer, i.e.,  $S1(+M_{FM}) \rightarrow S2(-M_{FM}) \rightarrow S3(+M_{FM})$ . Calculations show that the average orien-

tation of the AFM spins  $\langle \phi_{\text{AFM}} \rangle$  with respect to the direction  $\phi_{\text{H}} = 0^\circ$  acquires different values at states of  $S1$  and  $S3$  [21], because AFM spins switch irreversibly during the hysteresis loop of the FM layer. Accordingly, the angular dependence of  $\langle \phi_{\text{AFM}} \rangle$  at the state  $S1$  should show hysteresis between CW and CCW rotations, resulting in an altered magnetic state after CW and CCW rotations. This can be seen from the results at 300 K in Fig. 4(e). On setting the temperature of the AFM layer to 0 K, thereby removing the thermally activated transitions, the rotational hysteresis disappears. Therefore, the rotational hysteresis of the ADEB is suggested to be related to irreversible behavior of AFM spins and induced by thermal activation.

The discrepancy of  $H_{\text{E}}$  hysteresis between measured (Fig. 1(a)) and calculated (Fig. 4(a)) results can be explained as follows. The simulations assume a uniform AFM layer, while a wedge shaped sample is used in experiments. The magnetization reversal process is expected to be accompanied by motion of *single* domain wall for bilayers with wedged AFM layers [15], and by *multi-domain form* for uniform bilayers [22]. We have measured the ADEB of an FeNi/FeMn bilayer with uniform layers and found, as shown in Fig. 4(f)-4(i), the angular dependence of  $H_{\text{E}}$  to show hysteretic

behavior between CW and CCW rotations. Therefore, the disappearance of  $H_{\text{E}}$  hysteresis in Fig. 1(a) is caused by the wedged AFM layer and the associated magnetization reversal mechanism. Moreover, the present model can reproduce all features of uniform bilayers.

The features of the measured results in Fig. 3 can be qualitatively reproduced by the theoretical model, as analyzed below. For example, calculations have shown that for  $t_{\text{AFM}} = 2.5$  nm, 7 nm, and 10 nm,  $\Delta\phi_{\text{H}}$  is  $0^\circ$ ,  $7^\circ$ , and  $0^\circ$ , respectively, where the lateral size of AFM grains is 5.0 nm. At small  $t_{\text{AFM}}$ , all AFM grains are superparamagnetic, i.e., transitions are freely allowed between two stable states. Thus, the  $H_{\text{C}}$  enhancement and  $\Delta\phi_{\text{H}}$  are negligible. For large  $t_{\text{AFM}}$ , the AFM layer becomes thermally stable. However, some grains can be switched by the exchange field from the FM layer contributing a 'uniaxial' anisotropy which enhances  $H_{\text{C}}$  and induces  $\Delta\phi_{\text{H}}$ . For large enough  $t_{\text{AFM}}$ , the intrinsic energy barrier is increased further and  $p_{\text{sw}}$  is suppressed thereby decreasing  $H_{\text{C}}$  and  $\Delta\phi_{\text{H}}$ . Meanwhile, as the fraction of stable AFM grains increases,  $H_{\text{E}}$  increases monotonically. The behavior of  $H_{\text{E}}$  and  $H_{\text{C}}$  is well explained by the current model [23].

It is instructive to compare rotational hysteresis of torque with that of ADEB.

First, both reveal motion of AFM spins, in different ways [13]. Secondly, since the rotational hysteresis of torque also exists in single FM layers [24], it is not unique for FM/AFM bilayers. As a new experimental evidence, however, the hysteresis of the ADEB can exist *only* in FM/AFM bilayers because no such a phenomenon exists in single FM layers. As a new signature of the EB, the rotational hysteresis of the ADEB can better reflect the nature of the EB and the motion of AFM spins, in comparison with that of torque.

In summary, as a new signature of the EB, rotational hysteresis of the ADEB between CW and CCW rotations was studied for FeNi/FeMn bilayers. For small  $t_{\text{AFM}}$ , there is no hysteresis of the ADEB. It occurs for large  $t_{\text{AFM}}$  and increases with increasing  $t_{\text{AFM}}$  to reach a maximum. Finally it decreases. Calculations show that the average orientation of the AFM spins exhibits hysteresis during CW and CCW rotations. This arises from thermally activated transitions of the AFM grains. The remarkable agreement between theory and experiment gives strong support to the granular model of EB in polycrystalline bilayers.

**Acknowledgement** This work was supported by the National Science Foundation of China, National Key Projects for Basic Researches of China, Shanghai Science and

Technology Committee.

- 
- [1] J. Nogues and I. K. Schuler, J. Magn. Magn. Mater. **192**, 203(1999); A. E. Berkowitz and K. Takano, J. Magn. Magn. Mater. **200**, 552(1999)
  - [2] Z. P. Li et al, Phys. Rev. Lett. **96**, 217205(2006)
  - [3] B. Beckmann et al, Phys. Rev. Lett. **91**, 187201(2003)
  - [4] H. Ohldag et al, Phys. Rev. Lett. **91**, 017203(2003)
  - [5] W. Zhu et al, Phys. Rev. Lett. **86**, 5389(2001)
  - [6] A. Hoffmann, Phys. Rev. Lett. **93**, 097203(2004); M. D. Stiles and R. D. McMichael, Phys. Rev. B **59**, 3722(1999)
  - [7] A. Scholl et al, Phys. Rev. Lett. **92**, 247201(2004)
  - [8] C. L. Chien et al, Phys. Rev. B **68**, 014418(2003); F. Y. Yang and C. L. Chien, Phys. Rev. Lett. **85**, 2597(2000)
  - [9] J. Camarero et al, Phys. Rev. Lett. **95**, 057204(2005)
  - [10] E. Arenholz et al, Appl. Phys. Lett. **88**, 072503(2006)
  - [11] T. Ambrose et al, Phys. Rev. B **56**, 83(1997)
  - [12] O. de Haas et al, J. Magn. Magn. Mater. **260**, 380(2003)

- [13] M. Tsunoda et al, J. Appl. Phys. **87**, 4375(2000)
- [14] R. Nakatani, Jpn. J. Appl. Phys. **33**, 133(1994)
- [15] S. M. Zhou et al, Phys. Rev. B **58**, R14717(1998)
- [16] *Handbook of Discrete and Computational Geometry*, edited by J. E. Goodman and J. O'Rourke (CRC Press, New York, 1997).
- [17] R. W. Chantrell et al, Phys. Rev. B **63**, 24410(2000)
- [18] L. Néel, Ann. Geophys. (C.N.R.S) **5**, 99 (1949)
- [19] D. Mauri et al, J. Appl. Phys. **62**, 3047(1987)
- [20] E. Fulcomer and S. H. Charap, J. Appl. Phys. **43**, 4190(1972)
- [21] T. Hughes et al, J. Magn. Magn. Mater. **235**, 329(2001)
- [22] Z. Y. Liu and S. Adenwalla, Phys. Rev. B **67**, 184423(2003)
- [23] D. Choo et al, J. Appl. Phys. **101**, 09E521(2007)
- [24] I. S. Jacobs and F. E. Luborsky, J. Appl. Phys. **28**, 467(1957)

## FIGURE CAPTIONS

Figure 1 Measured angular dependence of  $H_E$  (a),  $H_C$  (b), normalized  $m_{y-AVE}/m_s$ (c), and asymmetric factor  $\delta$  (d) of FeNi(3 nm)/FeMn(10 nm) bilayer for CW and CCW rotations.  $m_s$  is the saturation magnetic moment of the sample.

Figure 2 Measured angular dependence of  $m_{y-AVE}/m_s$  for FeNi(3 nm)/FeMn(10 nm) in the  $\phi_H$  region of  $-30 \rightarrow 0 \rightarrow -30$  (a), and  $-30 \rightarrow 13 \rightarrow -30$ ,  $-30 \rightarrow 20 \rightarrow -30$ , and  $-30 \rightarrow 40 \rightarrow -30$  (b) in the unit of degrees.

Figure 3 Measured dependence of  $-H_E$  and  $H_C$  at  $\phi_H = 0^\circ$ (a) and  $\Delta\phi_H$  (b) on  $t_{AFM}$  for FeNi (3 nm)/FeMn bilayers. The solid lines serve a guide to the eye.

Figure 4 In left column, calculated angular dependence of  $H_E$  (a),  $H_C$  (b),  $m_{y-AVE}/m_s$  (c),  $\delta$  (d) at 300 K, and  $\langle \phi_{AFM} \rangle$  at the state  $S1$  throughout CW (squares) and CCW (circles) rotations at 0 K (solid symbols) and 300 K (open symbols) (e) of FM/AFM bilayer. In right column, measured angular dependence of  $H_E$  (f),  $H_C$  (g),  $m_{y-AVE}/m_s$  (h), and  $\delta$  (i) for typical *uniform bilayer* of FeNi (3 nm)/FeMn (7 nm).

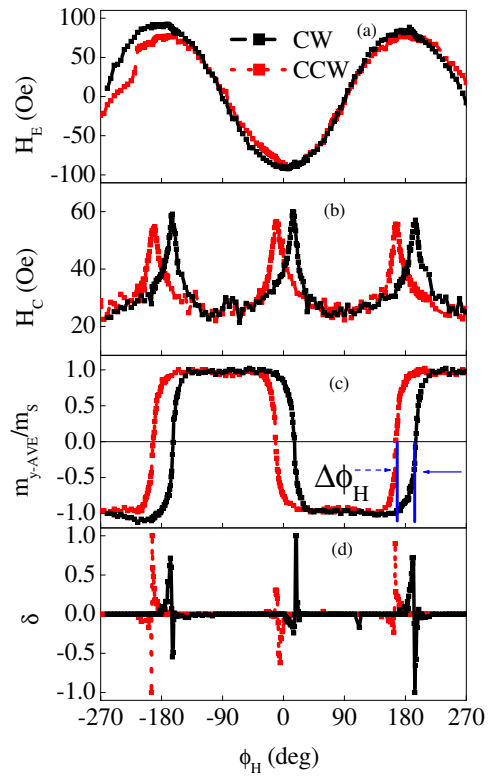


FIG. 1:

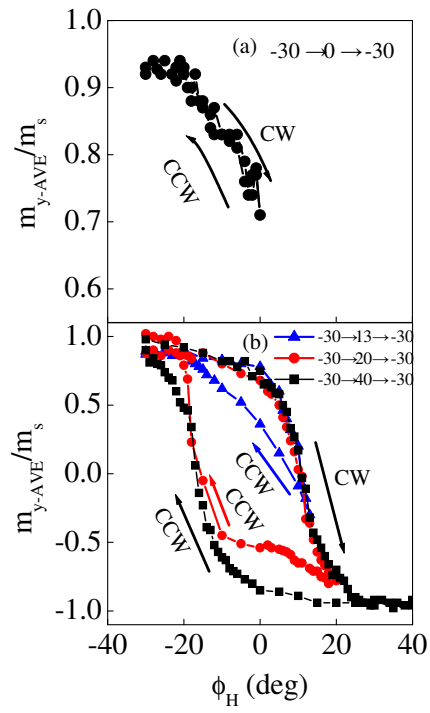


FIG. 2:

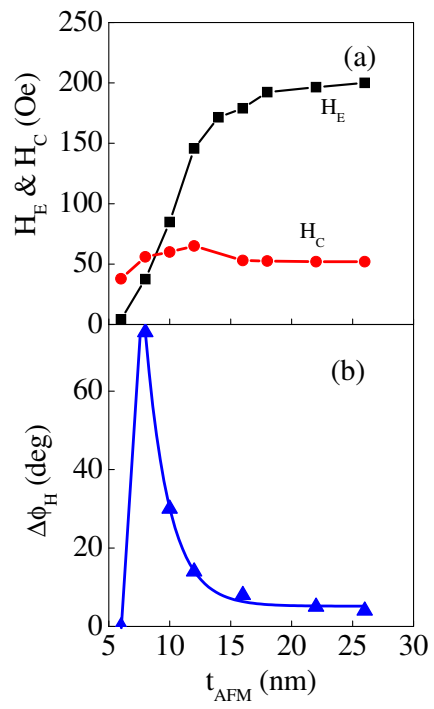


FIG. 3:

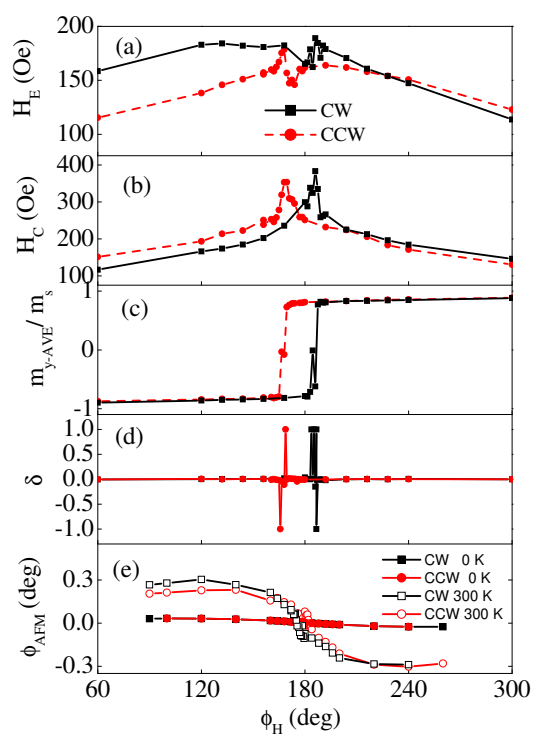


FIG. 4: